R. Maneiro-Catoira, J. Brégains, J. A. García-Naya and L. Castedo, "TMA–FDA Range-Angle Beamforming With Periodic Linear-Phase Time-Modulating Waveforms," in *IEEE Antennas and Wireless Propagation Letters*, vol. 21, no. 8, pp. 1602-1606, Aug. 2022, doi: 10.1109/LAWP.2022.3175107.

Link to published version: https://doi.org/10.1109/LAWP.2022.3175107

TMA-FDA Range-Angle Beamforming with Periodic Linear-Phase Time-Modulating Waveforms

Roberto Maneiro-Catoira, *Member, IEEE,* Julio Brégains, *Senior Member, IEEE,*
José A. García-Naya, *Senior Member, IEEE,* and Luis Castedo, *Senior Member, IEEE*

***Abstract*—Frequency diverse arrays (FDAs) provide range-angle time-invariant transmit-receive beamforming, although a fine focus of their radiation patterns is costly since high-resolution mixers and phase shifters are required. An innovative approach to FDAs is proposed in which mixers and phase shifters are replaced by the application of periodic linear-phase time-modulating waveforms to the antenna excitations implemented with 2-bit variable phase shifters controlled with periodic on-off instants of binary sequences, which leads to a simple and precise method for FDA beam focusing.**

***Index Terms*—Time-modulated arrays, frequency diverse arrays, beamsteering, beamforming.**

I. Introduction

THE so-called 4D arrays introduce an additional degree of freedom in antenna beamforming, namely time, in case of time-modulated arrays (TMAs), and frequency, in case of frequency diverse arrays (FDAs). Accordingly, FDAs synthesize time-range-angle dependent radiation patterns by applying frequency offsets to the individual array elements [1], while TMAs perform beamsteering (BS) by adjusting the on-off instants of the switches in their feeding network [2]–[12].

Since the FDA technique itself cannot generate range-dependent beampatterns in transmission [13], array signal processing is necessary at reception to activate the range-dependent property [14], thus allowing for the synthesis of dot-shaped time invariant diagrams in the range-angle space, i.e., the energy radiated by the antenna array is focused on a limited range-angle region during a certain time interval. This singular feature of FDAs to perform range-angle constrained transmit-receive beamforming is acquiring great potential in the radar and radio navigation arena [15], [16].

Existing FDA designs with collocated transmit-receive antennas [17], [18] utilize phase shifters and mixers whose resolution limit the FDA ability to perform continuous and accurate scanning or, if applicable, adaptive beamforming. This letter explores a different approach to FDA transmit-receive beamforming (BF) in which the antenna array excitations are synthesized by means of periodic phase modulations [19]–[21]. The benefits of the approach proposed are the following: 1) The use of low-complexity 2-bit phase shifters (consisting of 4 single-pole dual-throw (SPDT) switches) which avoids the use of mixers. 2) Beam steering with better resolution since both the FDA phases and frequency offsets can be adjusted continuously [8], [21]. This simply requires modifying the switch-on time instants of the periodic sequences that control the 2-bit phase shifters. An extra advantage is that the number of bits of the variable phase shifter (VPS) only determines the level of rejection of the unwanted harmonic beampatterns, thus achieving a suitable rejection level. 3) Additionally, and for the first time in architectures based on periodic phase modulations [19]–[21], the impact of the SPDT switches rise/fall times on both the level of rejection of the unwanted harmonics and the time-modulation radiation efficiency is analyzed.

* Corresponding author: José A. García-Naya (jagarcia@udc.es).

This work has been funded by the Xunta de Galicia (by grant ED431C 2020/15, and grant ED431G 2019/01 to support the Centro de Investigación de Galicia "CITIC"), the Agencia Estatal de Investigación of Spain (by grants RED2018-102668-T and PID2019-104958RB-C42) and ERDF funds of the EU (FEDER Galicia 2014-2020 & AEI/FEDER Programs, UE)

CITIC Research Center, University of A Coruña, 15071 A Coruña, Spain. E-mail: { roberto.maneiro, julio.bregains, jagarcia, luis.castedo}@udc.es.

Digital Object Identifier

II. Transmit-receive TMA-FDA system

Fig. 1 shows the block diagram of the collocated transmit-receive TMA-FDA system consisting of 1) a uniformly excited N-element transmit antenna array with an innovative TMA feeding network equipped with 2-bit VPSs and designed to work as an FDA; and 2) a single receive antenna followed by a signal processing chain based on the TMA technique.

A. Transmit signal model

We assume that the considered TMA-FDA system transmits the single-frequency signal $s(t) = e^{j2\pi f_c t}$, being f_c the carrier frequency (see Fig. 1). The excitation of each transmit antenna element is time-modulated with a periodic LP-TM waveform $p(t)$ having unit amplitude and a linear phase that varies from 0 to 2π during every period of duration T_0 (see Fig. 2a) or a good approximation to it. The simplest case consists in time-modulating the static excitations of a uniformly-excited linear array (ULA) with the same periodic signal $p(t)$. Note that $p(t)$ has only one spectral component at $q{=}+1$ (Fig. 2b). Thus, a single radiation pattern will appear at frequency $f_c + f_0$, with $f_0{=}1/T_0$. In this case, the positive first-order Fourier coefficient of $p(t)$, $P_1{=}1$, will become the excitation of each element in the corresponding array factor at $f_c{+}f_0$. Hence, a simple frequency translation of the ULA radiation pattern from f_c to $f_c{+}f_0$ is performed. Going one step further and considering time-shifted versions of $p(t)$ for each antenna element, $p(t - D_n)$, being D_n a variable time-delay, the corresponding positive first-order Fourier coefficient of $p(t - D_n)$ will have the form $e^{-j2\pi f_0 D_n}$. Since the phases of the positive first-order Fourier coefficients can be modified proportionally to

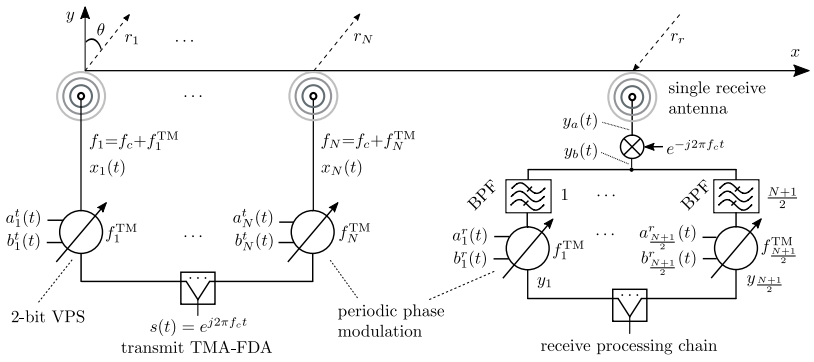

Fig. 1. Block diagram of the collocated transmit-receive antenna system for range-angle beamforming. The transmit TMA-FDA has N antenna elements while the receive processing chain has $(N+1)/2$ branches. Both transmit and receive systems are based on periodic phase modulation with 2-bit VPSs.

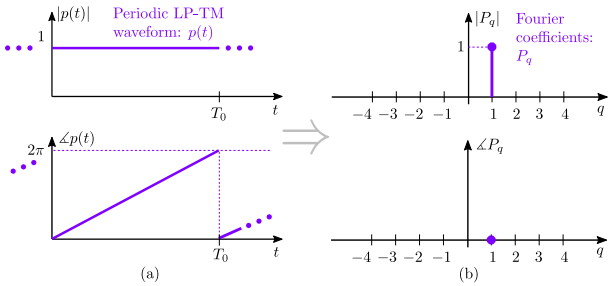

Fig. 2. Magnitude and phase of (a) the periodic extension of an LP-TM waveform $p(t)$; and (b) the corresponding Fourier coefficients. The only non-zero coefficient is at $q = +1$. If the slope of the phase were negative, it would be 2π for t=0 and zero for t=T_0, and the only spectral component would be at q=-1.

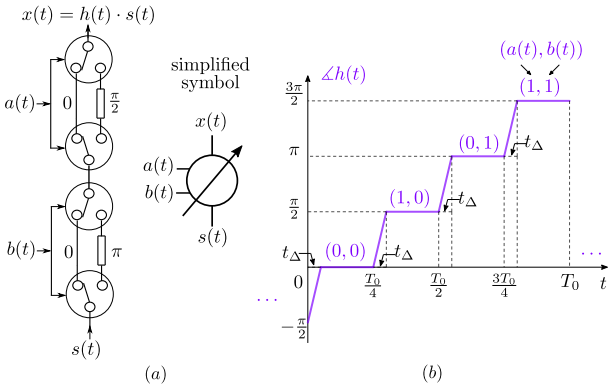

Fig. 3. (a) Layout with 4 SPDT switches (internal architecture of a 2-bit VPS governed by the binary signals $a(t)$ and $b(t)$) to synthesize $h(t)$, a 4-level quantized version of the LP-TM signal $p(t)$ in Fig. 2a. The input signal $s(t)$ is modulated by $h(t)$, yielding $x(t) = h(t) \cdot s(t)$. See also the simplified symbol that represents the switching architecture. (b) Synthesized $h(t)$ from the architecture in (a) for the 4 possible states of $a(t)$ and $b(t)$. Only $\angle h(t)$ is sketched since $|h(t)| = 1$. t_Δ denotes the rise/fall time of the SPDT switches.

the time delay D_n, the single harmonic pattern at f_c+f_0 can be steered to a given direction.

We next consider that the time-modulated (TM) fundamental frequency at the n-th element is different and given by

$$f_n^{\text{TM}} = f_0 + \Delta_{f_n}, \tag{1}$$

where Δ_{f_n} is the n-th antenna-element frequency-offset with respect to f_0. Hence, when also applying the time-delay D_n, the dynamic excitation of the n-th antenna element becomes $e^{-j2\pi f_n^{\text{TM}} D_n}$, which can be configured via f_n^{TM} and D_n.

This idea becomes more interesting when addressing its implementation with switches. Fig. 3a shows a layout with SPDT switches capable of generating $h(t)$, a 4-level quantized version of the signal $p(t)$ shown in Fig. 2a. Fig. 3b illustrates $\angle h(t)$, the quantized phase of $h(t)$, showing the phase level for each of the control signal values $a(t)$ and $b(t)$. Fig. 3b also includes the non-ideal rise/fall time of the switches, t_Δ. For the sake of simplicity, this non-ideal effect of the switches is modeled as a linear phase transient. Accordingly, given an interval A, if we define the indicator function χ_A as $\chi_A = 1$ if $x \in A$, and 0 otherwise, a single period of $h(t)$ is given by

$$\begin{aligned} h(t) &= e^{jm_\Delta\left(t-\frac{\pi}{2}\right)}\chi_{[0,t_\Delta)} + e^{j0}\chi_{[t_\Delta,T_0/4)} \\ &+ e^{jm_\Delta\left(t-\frac{T_0}{4}\right)}\chi_{[T_0/4,T_0/4+t_\Delta)} + e^{j\frac{\pi}{2}}\chi_{[T_0/4+t_\Delta,T_0/2)} \\ &+ e^{j\left[m_\Delta\left(t-\frac{T_0}{2}\right)+\frac{\pi}{2}\right]}\chi_{[T_0/2,T_0/2+t_\Delta)} + e^{j\pi}\chi_{[T_0/2+t_\Delta,3T_0/4)} \\ &+ e^{j\left[m_\Delta\left(t-\frac{3T_0}{4}\right)+\pi\right]}\chi_{[3T_0/4,3T_0/4+t_\Delta)} + e^{j\frac{3\pi}{2}}\chi_{[3T_0/4+t_\Delta,T_0)} \end{aligned} \tag{2}$$

with $m_\Delta = \pi/(2t_\Delta)$.

The time-modulation efficiency of the array is given by η_{TM}=$\mathcal{P}_U^{\text{TM}}/\mathcal{P}_R^{\text{TM}}$ [10] where $\mathcal{P}_U^{\text{TM}}$ and $\mathcal{P}_R^{\text{TM}}$ are the useful and total average power values radiated by the TMA, respectively. Note that η_{TM} accounts for the ability of a TMA to filter out and radiate only over the useful

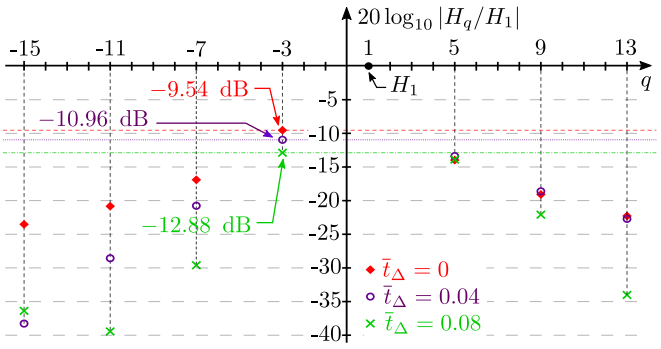

Fig. 4. Normalized Fourier series power spectrum of $h(t)$ (see Fig. 3c) considering three values of $\bar{t}_\Delta$=t_Δ/T_0 (normalized rise/fall time of the switches). The most meaningful undesirable harmonic corresponds to q=-3.

harmonics, in this case the first positive one. According to [22, Eq. 14], $\eta_{\text{TM}}=|H_1|^2/\sum_{q=-\infty}^{\infty}|H_q|^2$, with H_q being the Fourier coefficients of $h(t)$. Normalizing $h(t)$ such that $1/T_0\int_0^{T_0}|h(t)|^2dt=\sum_{q=-\infty}^{\infty}|H_q|^2=1$, a closed form expression for $\eta_{\text{TM}}=|H_1|^2$ is obtained:

$$\eta_{\text{TM}}=\left|\frac{1}{T_0}\int_0^{T_0}h(t)e^{-j\frac{2\pi t}{T_0}}dt\right|^2=\left|\frac{2-2je^{-2j\bar{t}_\Delta\pi}}{\pi-4\bar{t}_\Delta\pi}\right|^2, \quad (3)$$

a result that depends on the rise/fall time of the SPDT switches, $\bar{t}_\Delta$. In fact, for $\bar{t}_\Delta=\{0, 0.04, 0.08\}$ we obtain $\eta_{\text{TM}}=\{0.81, 0.86, 0.91\}$, and hence 81% to 91% of the total power corresponds to the first harmonic. This justifies $h_n(t)$, the n-th antenna LP-TM waveform, being approximated as

$$h_n(t)\approx H_1e^{-j2\pi f_n^{\text{TM}}D_n}e^{j2\pi f_n^{\text{TM}}t}, \quad 0\le t<T_0. \quad (4)$$

Fig. 4 plots $20\log_{10}|H_q/H_1|$, the normalized Fourier series power spectrum of $h(t)$, where it can be seen that the level of the most meaningful undesired harmonic at $q=-3$ is -9.54 dB, below that of the desired harmonic at $q=1$ in the ideal case $t_\Delta=0$, and even lower in the non-ideal cases in which the switches rise/fall times are not zero.

Accordingly, the signal transmitted by the n-th element of the TMA-FDA in Fig. 1 is

$$x_n(t)=h_n(t)e^{j2\pi f_ct}\approx H_1e^{-j2\pi f_n^{\text{TM}}D_n}e^{j2\pi(f_c+f_n^{\text{TM}})t} \quad (5)$$

Denoting

$$\varphi_n=-2\pi f_n^{\text{TM}}D_n, \text{ and } f_n=f_c+f_n^{\text{TM}} \quad (6)$$

and normalizing $x_n(t)$ with respect to H_1, we obtain

$$\overline{x}_n(t)\approx e^{j(2\pi f_nt+\varphi_n)}. \quad (7)$$

As in [22], [23], we consider that the frequency offsets in (1) have the form $\Delta_{f_n}=\Delta_f\cdot\Upsilon_n$, where Δ_f is a fixed frequency offset and

$$\Upsilon_n=\frac{1}{\beta_0(\alpha)}\beta_0\left(\alpha\sqrt{1-\left(\frac{2(n-(N+1)/2)}{N-1}\right)^2}\right)-1 \quad (8)$$

are the weights of a Kaiser window [24, Chapters 4 & 5] where α is a configuration parameter which allows for adjusting linearly the trade-off between sideband-lobe level (SLL) and half power beamwidth (HPBW), and $\beta_0(\cdot)$ is the modified Bessel function of the first kind and zero order. We will assume that N is odd to obtain a symmetric Kaiser window and, hence, the same Δ_{f_n} is applied to each pair of antenna elements with indices n and $N-(n-1)$. The central element with index $n=(N+1)/2$ will be the reference element with $\Delta_{f_n}=0$. Notice also that, according to (1) and the second equation in (6), symmetric frequency offsets Δ_{f_n} are properly applied to f_c+f_0, which is the frequency of the useful harmonic.

B. Signal processing at reception

Let us assume that the signal transmitted by the TMA-FDA is reflected on a target located at an arbitrary point with spatial coordinates (θ, r). The reflected signal, once collected by the receive antenna (see Fig. 1), will have the form [15]–[18]

$$y_a(t)=\sum_{n=1}^{N}e^{j\left(2\pi f_n\left(t-\frac{r_n}{c}-\frac{r_r}{c}\right)+\varphi_n\right)} \quad (9)$$

where c is the speed of light, $r_n\approx r-(n-1)d\sin(\theta)$ is the distance between the n-th element of the transmit antenna and the target (with d being the antenna element spacing), and $r_r\approx r$ is the distance between the target and the collocated receive antenna. Next, $y_a(t)$ is multiplied times $e^{-j2\pi f_ct}$ (see Fig. 1) and under the assumption –according to Fig. 4– that the level of unwanted harmonics is negligible, the following signal –see (6) and (7)– is obtained

$$y_b(t)=\sum_{n=1}^{N}e^{j[2\pi(f_n^{\text{TM}}t-f_n(\frac{r_n+r_r}{c}))+\varphi_n]} \quad (10)$$

As explained in Section II-A, due to the symmetry of Δ_{f_n}, $y_b(t)$ will have $(N+1)/2$ distinct spectral components. Since in a Kaiser window the minimum separation between two frequency offsets takes place between the center frequency and its adjacent frequency, we will employ bandpass filters (BPFs) (see Fig. 1) with bandwidth $\Delta_{f_{(N+1)/2}}-\Delta_{f_{(N-1)/2}}$ to ensure a correct filtering of the $(N+1)/2$ transmitted spectral components. If the index $k\in\{1,\ldots,(N+1)/2\}$ represents each branch of the receive chain in Fig. 1, we can express the signal at the output of each BPF as

$$y_k(t)=\begin{cases}e^{j\left[2\pi\left(f_k^{\text{TM}}t-f_k\left(\frac{r_i+r_r}{c}\right)\right)+\varphi_i\right]}+\\ +e^{j\left[2\pi\left(f_k^{\text{TM}}t-f_k\left(\frac{r_j+r_r}{c}\right)\right)+\varphi_j\right]}, & k\neq\frac{N+1}{2},\\ e^{j\left[2\pi\left(f_k^{\text{TM}}t-f_k\left(\frac{r_k+r_r}{c}\right)\right)+\varphi_k\right]}, & k=\frac{N+1}{2}\end{cases} \quad (11)$$

with $i+j=N+1$.

We next time-modulate each BPF output $y_k(t)$ with a periodic LP-TM signal $h_k(t)$ similar to the one in (4), but with negative slope (see the caption of Fig. 2). Instead of an ascending staircase (see Fig. 3c), we apply a descending one with $D_k=0$ and obtain the following constant signal[1]

$$y_k\approx H_1e^{-j2\pi f_k^{\text{TM}}t}y_k(t), \quad 0\le t<T_0. \quad (12)$$

Normalizing (12) with respect to H_1, and considering that the level of the unwanted harmonics is negligible, we obtain

$$\overline{y}_k=\begin{cases}e^{j\left(\frac{-2\pi f_k(r_i+r_r)}{c}+\varphi_i\right)}+\\ +e^{j\left(\frac{-2\pi f_k(r_j+r_r)}{c}+\varphi_j\right)}, & k\neq\frac{N+1}{2},\\ e^{j\left(\frac{-2\pi f_k(r_k+r_r)}{c}+\varphi_k\right)}, & k=\frac{N+1}{2}\end{cases} \quad (13)$$

and we can observe that the time-variant character (inherent to any transmit FDA) is removed by using LP-TM quantized waveforms at reception. We highlight that the Kaiser window symmetry allows us to use only $(N+1)/2$ BPFs (similar to the symmetric logarithm frequency offsets in [15]) but, in addition, the use of periodic LP-TM signals yields BPFs with center

[1]For the sake of simplicity, in this letter we consider null time delays at reception. However, non-zero delays could be considered (without additional hardware) to optimize the transmit-receive diagram, in the same way that phase shifters are used in [15], [17], [18].

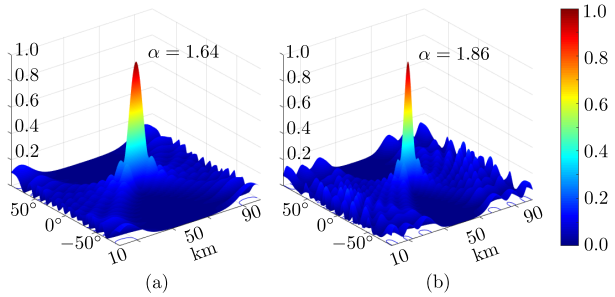

Fig. 5. Normalized 3-D transmit-receive beampatterns with N=21, Δ_f=10 kHz, (r_0, θ_0)=(50 km, 0°), and: (a) α=1.64; (b) α=1.86. The Kaiser window configuration parameter α allows for the adjustment of the trade-off between SLL and HPBW [24, Chapter 5].

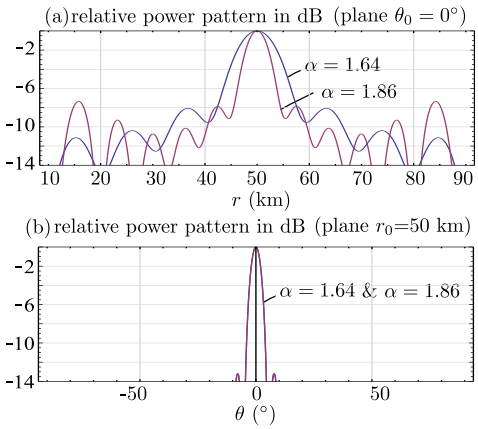

Fig. 6. For the beampatterns in Fig. 5a and Fig. 5b: (a) θ_0-plane cuts for α=1.64 (HPBW$_r$=9.2 km and SLL$_r$= − 8.24 dB) and α=1.86 (HPBW$_r$=5.3 km and SLL$_r$= − 7.45 dB); (b) r_0-plane cuts which are not sensitive to α and yield HPBW$_\theta$=4.8° and SLL$_\theta$= − 13.2 dB.

frequencies in the order of f_0, with $f_0 \ll f_c$. Therefore, our proposal exhibits a fractional bandwidth (FBW) much more affordable than those proposed in [15], [17].

C. TMA-FDA transmit-receive beamforming

In view of (1), (6), and (13), the array factor of the collocated transmit-receive TMA-FDA system in Fig. 1 is

$$F_A(r,\theta) = \sum_{k=1}^{(N+1)/2} \overline{y}_k = \sum_{n=1}^{N} e^{j\left(\frac{-2\pi f_n (r_n + r_r)}{c} + \varphi_n\right)} = \\ = \sum_{n=1}^{N} e^{j\left(\frac{-2\pi (f_c + f_0 + \Delta f_n)(2r - (n-1)d\sin\theta)}{c} + \varphi_n\right)} \quad (14)$$

Since $\max(\Delta_{f_n}) \ll (f_c + f_0)$, the array factor expression (in the same way as in [15], [16], [18], [25]–[28]) simplifies to

$$F_A(r,\theta) = \sum_{n=1}^{N} e^{j\left(\frac{2\pi}{c}[(n-1)d(f_c+f_0)\sin\theta - 2f_n r] + \varphi_n\right)}. \quad (15)$$

Accordingly, the useful harmonic beampattern at $f_c + f_0$ can be steered towards a target with spatial coordinates (r_0, θ_0), generating a maximum value in the power radiated beampattern. Indeed, by adjusting

$$\varphi_n = -(2\pi/c)\,[(n-1)d(f_c + f_0)\sin\theta_0 - 2f_n r_0] \quad (16)$$

TABLE I
SLL COMPARISON FOR DIFFERENT TRANSMIT-RECEIVE FDAS WITH UNIFORM WEIGHT VECTORS AT THE RECEIVER.

Transmit-receive FDA	SLL$_\Omega$ (dB)	SLL$_r$ (dB)	SLL$_\theta$ (dB)
SLFO1 [15]	-4.85	-7.80	-13.20
SLFO2 [15]	-6.27	-7.00	-13.20
MSLFO1 [15]	-4.49	-11.00	-13.20
MSLFO2 [15]	-5.42	-10.20	-13.20
This work (α=1.64)	-6.02	-8.24	-13.20

the array factor takes the form

$$F_A(r,\theta) = \sum_{n=1}^{N} e^{j\left(\frac{2\pi}{c}[(n-1)d(f_c+f_0)(\sin\theta - \sin\theta_0) - 2f_n(r-r_0)]\right)} \quad (17)$$

which means that we can select φ_n so that the maximum of the radiation pattern points towards the target.

III. Numerical Examples

Considering an observation region Ω=$\{r$∈$[10\,\text{km}, 90\,\text{km}]$, θ∈$[-90°, 90°]\}$, Fig. 5 plots the resulting time-invariant dot-shaped beam patterns obtained with the proposed transmit-receive TMA-FDA system for a target position (r_0, θ_0)=(50 km, 0°). We considered f_c=10 GHz, f_0=1 MHz, Δ_f=10 kHz, $d = \lambda_c/2$ (with λ_c being the carrier wavelength), and two values of α (α=1.64 and α=1.86) to illustrate its usefulness to adjust the trade-off between SLL and HPBW. To quantify this feature, the caption of Fig. 6 provides the resulting values for the SLL and HPBW in the corresponding θ_0 and r_0 plane cuts for the two values of α.

Table I shows the comparison in terms of SLL between the FDA approaches symmetric logarithmically increasing frequency offset (SLFO) [15] and modified symmetric logarithmically increasing frequency offset (MSLFO) [15] which are equivalent to the one proposed in this letter. Both the proposed TMA-FDA and SLFO2 exhibit the best SLL$_\Omega$ over the whole observation area Ω, but with the advantage that the SLL$_r$ (θ_0 cut) improves over the SLL$_\Omega$ by 36.7% for the proposed TMA-FDA, whereas such improvement is only 11.6% for SLFO2.

IV. Conclusions and Future Work

We have presented an innovative transmit-receive TMA-FDA approach governed by periodic LP-TM waveforms which is able to synthesize time-invariant dot-shaped beampatterns in the range-angle domain. The application of a highly efficient TMA scheme to accomplish FDA features enables a simple array architecture that uses 2-bit phase shifters and SPDT switches instead of more expensive high resolution VPS and mixers. While the results of this analysis are promising, we are aware that there are future lines of research yet to be addressed. The next advances are the realization of full-wave simulations, and the construction and characterization of a hardware prototype.

REFERENCES

[1] P. Antonik, M. C. Wicks, H. D. Griffiths, and C. J. Baker, "Frequency diverse array radars," in *2006 IEEE Conference on Radar*, 2006, pp. 215–217.

[2] P. Rocca, Q. Zhu, E. T. Bekele, S. Yang, and A. Massa, "4-d arrays as enabling technology for cognitive radio systems," *IEEE Transactions on Antennas and Propagation*, vol. 62, no. 3, pp. 1102–1116, 2014.

[3] P. Rocca, G. Oliveri, R. J. Mailloux, and A. Massa, "Unconventional phased array architectures and design methodologies—a review," *Proceedings of the IEEE*, vol. 104, no. 3, pp. 544–560, 2016.

[4] L. Poli, P. Rocca, G. Oliveri, and A. Massa, "Harmonic beamforming in time-modulated linear arrays," *IEEE Trans. Antennas Propag.*, vol. 59, no. 7, pp. 2538–2545, Jul. 2011.

[5] G. Li, S. Yang, Y. Chen, and Z.-P. Nie, "A novel electronic beam steering technique in time modulated antenna array," *Progress In Electromagnetics Research*, vol. 97, pp. 391–405, 2009.

[6] Y. Tong and A. Tennant, "A two-channel time modulated linear array with adaptive beamforming," *IEEE Trans. Antennas Propag.*, vol. 60, no. 1, pp. 141–147, Jan 2012.

[7] A. M. Yao, W. Wu, and D. G. Fang, "Single-sideband time-modulated phased array," *IEEE Trans. Antennas Propag.*, vol. 63, no. 5, pp. 1957–1968, May 2015.

[8] Q. Chen, J. Zhang, W. Wu, and D. Fang, "Enhanced single-sideband time-modulated phased array with lower sideband level and loss," *IEEE Trans. Antennas Propag.*, vol. 68, no. 1, pp. 275–286, Jan. 2020.

[9] H. Li, Y. Chen, and S. Yang, "Harmonic beamforming in antenna array with time-modulated amplitude-phase weighting technique," *IEEE Transactions on Antennas and Propagation*, vol. 67, no. 10, pp. 6461–6472, 2019.

[10] R. Maneiro Catoira, J. Brégains, J. A. Garcia-Naya, L. Castedo, P. Rocca, and L. Poli, "Performance analysis of time-modulated arrays for the angle diversity reception of digital linear modulated signals," *IEEE J. Sel. Topics Signal Process.*, vol. 11, no. 2, pp. 247–258, Mar. 2017.

[11] G. Bogdan, K. Godziszewski, Y. Yashchyshyn, C. H. Kim, and S. Hyun, "Time modulated antenna array for real-time adaptation in wideband wireless systems- part I: Design and characterization," *IEEE Trans. Antennas Propag.*, pp. 1–1, 2019.

[12] R. Maneiro-Catoira, J. Brégains, J. A. García-Naya, and L. Castedo, "Time modulated arrays: From their origin to their utilization in wireless communication systems," *Sensors*, vol. 17, no. 3, pp. 1–14, Mar. 2017.

[13] M. Fartookzadeh, "Comments on "combining switched tmas and fdas to synthesize dot-shaped beampatterns"," *IEEE Antennas and Wireless Propagation Letters*, vol. 20, no. 12, pp. 2559–2559, 2021.

[14] W. Wang, "Retrodirective frequency diverse array focusing for wireless information and power transfer," *IEEE Journal on Selected Areas in Communications*, vol. 37, no. 1, pp. 61–73, 2019.

[15] Y. Xu and K.-M. Luk, "Enhanced transmit–receive beamforming for frequency diverse array," *IEEE Transactions on Antennas and Propagation*, vol. 68, no. 7, pp. 5344–5352, 2020.

[16] M. Tan, C. Wang, and Z. Li, "Correction analysis of frequency diverse array radar about time," *IEEE Transactions on Antennas and Propagation*, vol. 69, no. 2, pp. 834–847, 2021.

[17] Y. Xu and J. Xu, "Corrections to "range-angle-dependent beamforming of pulsed-frequency diverse array" [jul 15 3262-3267]," *IEEE Transactions on Antennas and Propagation*, vol. 66, no. 11, pp. 6466–6468, 2018.

[18] Y. Xu, X. Shi, W. Li, J. Xu, and L. Huang, "Low-sidelobe range-angle beamforming with fda using multiple parameter optimization," *IEEE Transactions on Aerospace and Electronic Systems*, vol. 55, no. 5, pp. 2214–2225, 2019.

[19] Y. Gao, G. Ni, K. Wang, Y. Liu, C. He, R. Jin, and X. Liang, "Single-sideband time-modulated phased array with 2-bit phased shifters," in *2020 9th Asia-Pacific Conference on Antennas and Propagation (APCAP)*, 2020, pp. 1–2.

[20] G. Ni, L. Zhang, Y. Gao, C. He, J. Chen, and R. Jin, "High-efficiency harmonic beamforming with multi-branch time-modulated array," in *2021 15th European Conference on Antennas and Propagation (EuCAP)*, 2021, pp. 1–4.

[21] Q. Zeng, P. Yang, L. Yin, H. Lin, C. Wu, F. Yang, and S. Yang, "Phase modulation technique for harmonic beamforming in time-modulated arrays," *IEEE Transactions on Antennas and Propagation*, pp. 1–1, 2021.

[22] R. Maneiro-Catoira, J. Brégains, J. A. García-Naya, and L. Castedo, "Combining switched TMAs and FDAs to synthesize dot-shaped beampatterns," *IEEE Antennas and Wireless Propagation Letters*, vol. 20, no. 9, pp. 1716–1720, 2021.

[23] ——, "A TMA-FDA approach for two-beam steering," *IEEE Antennas and Wireless Propagation Letters*, vol. 20, no. 10, pp. 1973–1977, 2021.

[24] K. Prabhu, *Window Functions and Their Applications in Signal Processing (1st ed.)*. CRC Press, 2014.

[25] M. Secmen, S. Demir, A. Hizal, and T. Eker, "Frequency diverse array antenna with periodic time modulated pattern in range and angle," in *2007 IEEE Radar Conference*, 2007, pp. 427–430.

[26] A. Basit, I. M. Qureshi, W. Khan, S. u. Rehman, and M. M. Khan, "Beam pattern synthesis for an fda radar with hamming window-based nonuniform frequency offset," *IEEE Antennas and Wireless Propagation Letters*, vol. 16, pp. 2283–2286, 2017.

[27] W. Wang, H. C. So, and A. Farina, "An overview on time/frequency modulated array processing," *IEEE Journal of Selected Topics in Signal Processing*, vol. 11, no. 2, pp. 228–246, 2017.

[28] W.-Q. Wang, "Overview of frequency diverse array in radar and navigation applications," *IET Radar, Sonar & Navigation*, vol. 10, pp. 1001–1012(11), July 2016. [Online]. Available: https://digital-library.theiet.org/content/journals/10.1049/iet-rsn.2015.0464